





Periodic Leaky-Wave Antenna With Circular Polarization and Low-SLL Properties

Xingying Huo , Junhong Wang, *Senior Member, IEEE*, Zheng Li , Yujian Li , Meie Chen, and Zhan Zhang 

Abstract—A periodic leaky-wave array antenna with circular polarization and low sidelobe level (SLL) for millimeter-wave application is proposed. The unit cell of the array consists of four circular split rings located on both sides of a low-loss substrate, and a planar Goubau line is used to excite the split rings to generate radiation. The antenna can realize an impedance bandwidth larger than 67%, and the 3 dB axial-ratio bandwidth is about 8.9%. The maximum gain is about 18 dBi. To reduce the SLL, the leakage loss factor α along the radiation aperture is tapered, using beam-forming technique, by controlling the aperture field distribution into a cosine function. The results show that the SLL of the proposed antenna is about 6 dB lower than that of the antenna with uniform aperture field distribution. The antenna was fabricated and measured, and the experimental results are in good agreement with those of simulation.

Index Terms—Circular polarization, circular split ring, leaky-wave antenna (LWA), low sidelobe level (SLL), periodic structure.

I. INTRODUCTION

CIRCULARLY polarized (CP) antenna attracts more and more interests and becomes an indispensable part of many wireless communication systems for two advantages: One is that the CP antenna is more immune to the “Faraday rotation” effect caused by the ionosphere [1], which has significant effect on the satellite communication [2] and radar systems [3]; the other is that it can reduce multipath effect and polarization mismatch in complicated environments [4], [5]. In the past decades, applications in millimeter-wave bands have received comprehensive attention [6], [7], and many new kinds of CP antennas in these frequency bands have been proposed, such as magnetoelectric dipole CP antenna [8], cavity-backed CP antennas [9], CP patch antenna [10], CP helical antenna [11], CP grid antenna [12], and CP open-loop antenna [13].

When designing CP antennas, microstrip line is one of the most frequently used transmission structures because of its low profile, light weight, and easy fabrication, but its radiation attenuation results in low efficiency of the antenna [14], and both the dielectric and ohmic losses are increasing significantly in high-frequency band [15]. Thus, the planar Goubau line (PGL)

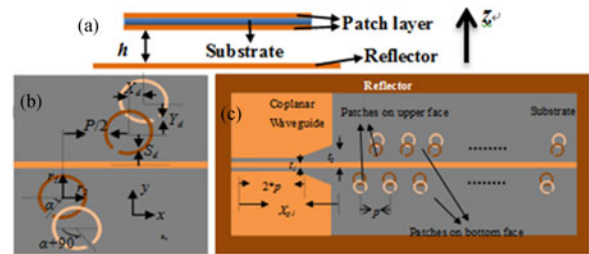


Fig. 1. Configuration and parameters of the CP LWA: (a) Side view, (b) top view, and (c) unit cell of the complete model.

is chosen as the transmission structure in this letter, which consists of a strip line without ground and could reduce the dielectric and ohmic losses significantly, since the field is not highly confined in the dielectric substrate any more [16].

In this letter, a new periodic leaky-wave antenna (LWA) with low sidelobe level (SLL) and high radiation efficiency is designed based on a PGL for CP radiation. The radiation structure consists of two sets of circular split rings located on each side of the PGL's dielectric substrate, as shown in Fig. 1. The two sets of rings are placed orthogonally in terms of the split slots cut in the rings, for reducing the cross polarization. Since the Goubau transmission line is a single-conductor line not compatible with the SMA connector, a smooth transition into 50 Ω coplanar waveguide is designed for both impedance transformation and mode conversion [17]. The structure could radiate in both sides of the substrate, so in order to obtain a single beam radiation, a reflector is placed behind the substrate by a distance of h , as shown in Fig. 1(a). The low SLL is realized by adjusting the deviations between the split rings and the central strip in a meandering way. There are a total of ten periods of circular split rings, distributed alternatively on both sides of the PGL's central metallic strip. CST Microwave Studio is used in the simulation for analyzing the antenna property.

II. CIRCULARLY POLARIZED PERIODIC LEAKY WAVE ANTENNA (CP-PLWA)

A. Structure and Mechanism

Fig. 1(b) gives the top view of the whole structure of the proposed CP-PLWA. The classical PGL, with a metallic strip along the centerline on upper surface of the dielectric substrate, is used as the basic feeding structure of the antenna. Since the radiation from fundamental mode is suppressed [18], periodic patches are designed to generate radiation from the spatial harmonics.

Fig. 1(c) shows the unit cell of the CP-PLWA, which consists of four circular split rings, divided into two sets. One set is on the upper side of the substrate with a rotation angle of α

Manuscript received March 27, 2018; revised May 15, 2018; accepted May 16, 2018. Date of publication May 21, 2018; date of current version July 4, 2018. This work was supported in part by the Fundamental Research Funds for the Central Universities under Grant W16JB00020 and in part by the National Natural Science Foundation of China under Grant 61331002. (Corresponding author: Junhong Wang.)

The authors are with the Key Laboratory of All Optical Network and Advanced Telecommunication Network of the Ministry of Education, Institute of Lightwave Technology, Beijing Jiaotong University, Beijing 100044, China (e-mail: 13111003@bjtu.edu.cn; wangjunh@bjtu.edu.cn; lizheng@bjtu.edu.cn; liyujian@bjtu.edu.cn; mechen@bjtu.edu.cn; zhangzhan@bjtu.edu.cn).

Digital Object Identifier 10.1109/LAWP.2018.2838576

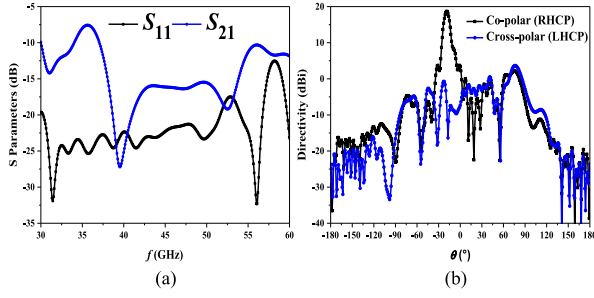


Fig. 2. Simulated results of the CP-PLWA for (a) S -parameters and (b) copolar and cross-polar components of the radiation pattern in the xz plane at 45 GHz.

(in terms of split slots cut in the circular rings), and another is on the lower side with a rotation angle of $\alpha + 90^\circ$. The longitudinal and transverse distances of the two orthogonal circular split rings on opposite sides of the substrate are denoted, respectively, by X_d and Y_d , and the distance from the center of the circular split rings on upper side to the central strip is denoted by S_d , which mainly controls the attenuation level (coupled power), and, consequently, determines the radiation efficiency. As is well known, a circular-polarization plane wave can be generated by two orthometric field components with the same amplitudes and a phase difference of 90° . In this structure, the amplitudes of the two orthometric aperture fields can be adjusted by the rotation angles α , and the 90° phase shift can be realized by adjusting the thickness of the substrate H_s and the longitudinal and transverse distances between the two orthogonal circular split rings: X_d and Y_d .

There are totally ten periods contained in the complete CP antenna. To produce a single radiation beam from the -1 st spatial harmonic, the period of the patches is selected to $p = 4.7$ mm ($0.7\lambda_0$). In this leaky-wave structure, patches on both sides of the substrate can radiate in opposite directions, but with opposite polarizations [right-hand circularly polarized (RHCP) or left-hand circularly polarized (LHCP)]. Therefore, the reflector is not only acting as a reflector, but also acting as an effective polarizer, so a single upward CP beam can be obtained, and the antenna gain is enhanced.

B. Results and Analysis

The proposed antenna is simulated and optimized at $f = 45$ GHz. The permittivity and loss tangent of the substrate are $\epsilon_r = 1.8$ and $\tan \delta = 0.02$, which is taken from [16]. The loss tangent is maybe a little bit higher for millimeter-wave application, but the radiating characteristics of the antenna do not change too much. The size of the substrate is $30 \text{ mm} \times 68 \text{ mm} \times 0.4 \text{ mm}$. The reflector is set with the same center as substrate, but 5 mm wider and 10 mm longer than the substrate, and is placed 5 mm away from the substrate. Radius of the circular rings r_1 and r_2 is set to 1.1 and 0.94 mm, respectively, and the width of the split W_d is set to 0.3 mm. Other parameters are $S_d = 2$ mm, $\alpha = 65^\circ$, $X_d = 0.1$ mm, $Y_d = 1.4$ mm, $t_1 = 0.625$ mm, $t_2 = 1.625$ mm, and $X_{p1} = 15$ mm. Fig. 2(a) shows the simulated S -parameters of the CP-PLWA. A wave port is vertically located at the end of the antenna as the port 2 for computing S_{21} . It indicates that the impedance bandwidth is larger than 67% for $S_{11} < -10$ dB at the center frequency of 45 GHz and the efficiency is over 90% within the whole U-band. Comparison for the copolar (RHCP) and cross-polar

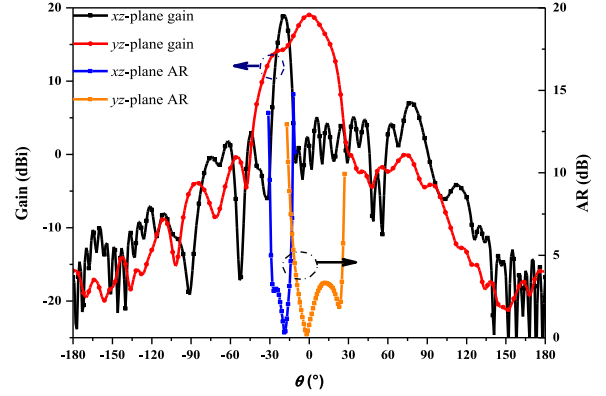


Fig. 3. Simulated results for the radiation pattern and AR in both yz plane and xz plane at 45 GHz.

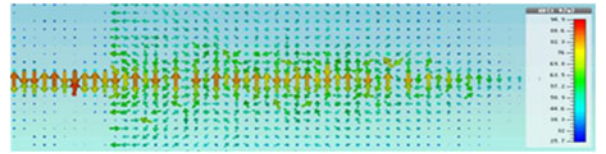


Fig. 4. Distributions of the surface electric fields on the CP-PLWA

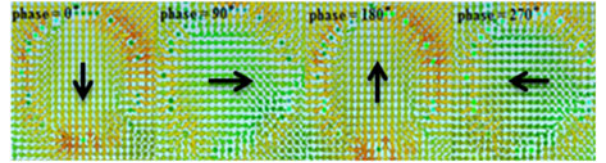


Fig. 5. Electric field in the aperture of one circular split ring with different feeding phases.

(LHCP) components of the radiation pattern in the xz plane at 45 GHz is given in Fig. 2(b), showing that the cross-polar component (-6.3 dBi) is 25 dB lower than the copolar component (18.7 dBi) in the main beam direction.

The simulated results of the gain pattern and the AR of the antenna at 45 GHz are given in Fig. 3. It shows that the proposed antenna has a good CP property in both xz plane and yz plane around the main beam, which indicates the quality of the CP radiation.

Fig. 4 gives the distribution of the near electric fields along the aperture of the proposed antenna. It is found that the power propagating along the antenna is similar to a traveling wave, and the radiation is generated mainly from the circular split rings. Fig. 5 gives the near electric field distribution in the aperture of one circular split ring with different feeding phases. The direction of the electric field is found rotating anticlockwise with changing phase, which verifies the generation of CP radiation.

Fig. 6 shows the simulated results of both the gain and axial ratio (AR) of the CP-PLWA as functions of θ for different frequencies. It is indicated that the beamwidth and antenna gain change little (about 8° and 18.2 dBi, respectively) when frequency increases from 42.5 to 46.5 GHz. Meanwhile, the AR within the main beam shows a good property within the frequency band, and the AR is less than 1 dB within the main beam at 45 GHz.

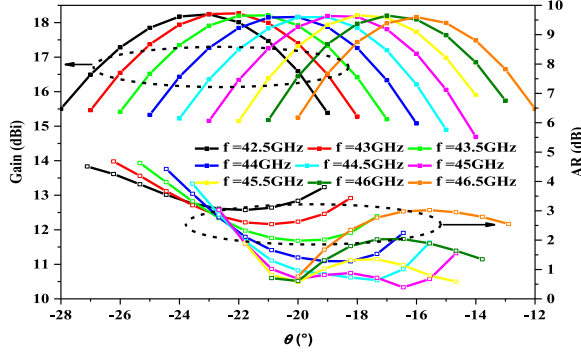
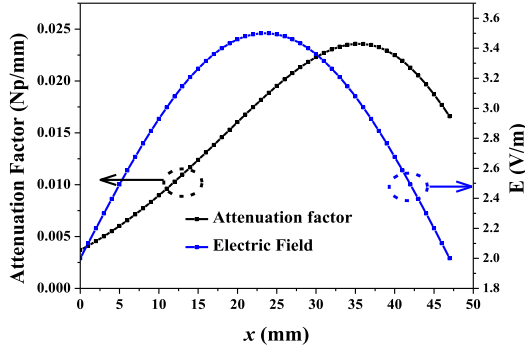
Fig. 6. Simulated results for gain and AR in the xz plane for different f .

Fig. 7. Distributions of the tapered attenuation factor and the electric field along the antenna.

III. MODIFICATION OF THE ANTENNA STRUCTURE FOR LOW SLL

A. Theory and Method

As we know, to realize the low-SLL property of an antenna, the aperture field distribution should be designed as a cosine function [18]. For the structure of antenna proposed in this letter, the field strength in the aperture varies with the increasing of the half aperture width S_d . The accurate variation function between the deviation of patches and aperture field distribution $E(x)$ is hard to be established directly [19], but the leakage factor distribution $\alpha(x)$ could be computed through the aperture field distribution approximately [20]

$$2\alpha(x) = |E(x)|^2 / \left[\left(\frac{1}{1-R} \right) \int_0^{L_s} |E(\xi)|^2 d\xi - \int_0^l |E(\xi)|^2 d\xi \right] \quad (1)$$

where l is the distance from the origin to the considering point in the aperture, and R denotes the proportion of power absorbed by the load, calculated by $R = |S_{21}|^2$. The average value of R for different aperture deviations is approximately used in (1). Using this approximation, the designing procedure is significantly simplified.

B. Design and Results

In this letter, the aperture field is designed to be the cosine distribution

$$E(x) = 1.5 \cos \left(\frac{\pi}{47} x - \frac{\pi}{2} \right) + 2. \quad (2)$$

Thus, the distribution of $\alpha(x)$ could be carried out from (1) and (2), and the results are shown in Fig. 7. The distribution of

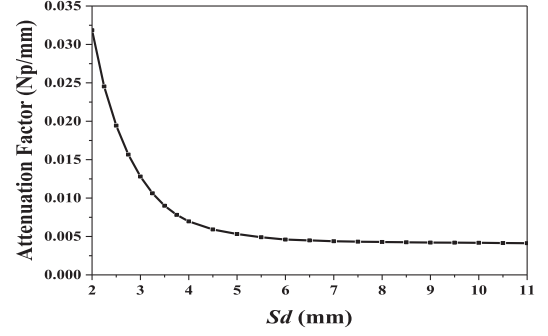
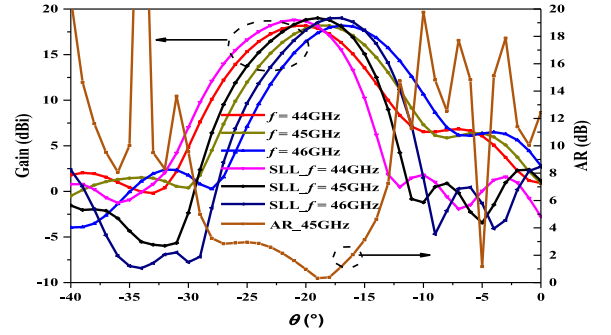
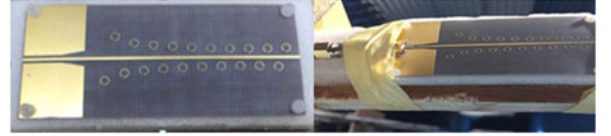
Fig. 8. Attenuation factors as functions of S_d .Fig. 9. Gain of the antenna for different f and AR at 45 GHz as function of θ .

Fig. 10. Photographs of the fabricated antenna.

$\alpha(x)$ along the antenna presents an asymmetrical cosine curve since the power is radiated and attenuated along the PGL, which explains why S_d is not minimized in the center of the structure. Fig. 8 gives the distribution of $\alpha(x)$ as function of the half aperture width S_d , which indicates that the coupled power decreases with the increasing of aperture width. According to this variation curve, a ten-unit-cells CP-PLWA is designed with the electric field distribution tapered as a cosine function by changing S_d , and an antenna with low-SLL property is realized. Fig. 9 gives the comparison between the radiation patterns of the designed low-SLL CP-PLWA and the antenna with uniform aperture width of $S_d = 2$ mm for different frequencies, indicating that the SLL of the proposed antenna is at least 6 dB lower within the frequency band. Fig. 9 also gives the AR of the low-SLL CP-PLWA at central frequency, which illustrates that the proposed antenna keeps a good CP property at 45 GHz.

The above proposed low-SLL CP-PLWA was fabricated, and the photograph of the antenna is shown in Fig. 10. Four screws are used to fix the antenna together, with a piece of cuboid-shaped foam between the substrate and reflector. Fig. 11(a) gives the simulated and measured results of S_{11} , indicating a good impedance matching of the antenna. Fig. 11(b) gives the comparison of the simulated and measured radiation patterns in the xz plane at 45 GHz, which shows a good agreement in main beam and SLL of the near-side lobes, but for the far-side lobes, the measured results are not as good as those of simulation. Although the test is conducted in an anechoic chamber, the

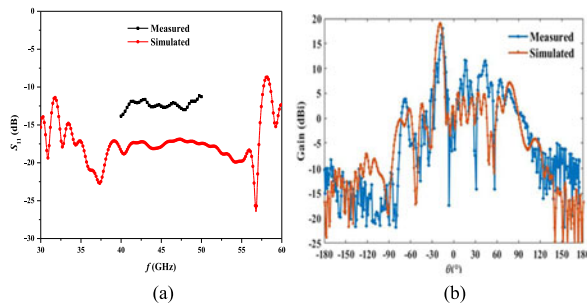


Fig. 11. Simulated and measured results for (a) S-parameters and (b) realized gain of the low-SLL CP-PLWA in the xz plane.

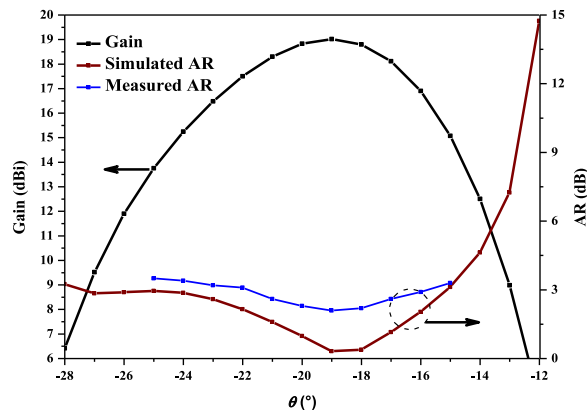


Fig. 12. Simulated and measured AR at 45 GHz and simulated gain as function of θ .

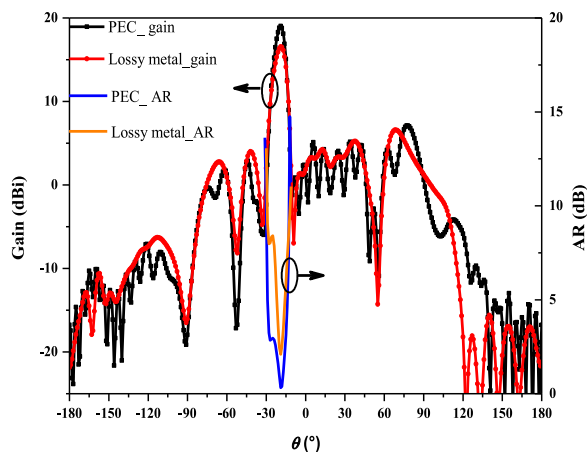


Fig. 13. Simulated results for the radiation pattern and AR with and without the practical metallic loss in the xz plane at 45 GHz.

weak-side lobe of the antenna is still easier to be affected by the environment at high frequency.

The AR is measured just around the main beam, due to the limited condition of the test system, and Fig. 12 compares the simulated and measured results of AR, which shows a general agreement. Thus, realized gain and AR are compared for the antenna with practical metallic losses in the xz plane, as shown in Fig. 13. The results show that the realized gain decreases by about 1 dB with the metallic loss. The AR of the antenna with metallic losses is also worsened by 1 dB, but it could still produce a CP radiation around the main beam.

IV. CONCLUSION

In this letter, a CP LWA with low SSL is proposed and designed based on the PGL. A new kind of circular split ring is designed for radiating a CP wave, and a tapering aperture field distribution is used to realize the low SLL. The 3 dB AR bandwidth of the proposed antenna is about 8.9%, and the SLL is reduced about 6 dB at the central frequency. The efficiency of the antenna is over 90%, and measured results are in agreement with simulated results.

REFERENCES

- [1] E. Brookner *et al.*, "Faraday loss for L-band radar and communications systems," *IEEE Trans. Aerosp. Electron. Syst.*, vol. AES-21, no. 4, pp. 459–469, Jul. 1985.
- [2] E. Arneri *et al.*, "A compact high gain antenna for small satellite applications," *IEEE Trans. Antennas Propag.*, vol. 55, no. 2, pp. 277–282, Feb. 2007.
- [3] Y. V. Vissan *et al.*, "Development of circularly polarized array antenna for synthetic aperture radar sensor installed on UAV," *Prog. Electromagn. Res. C*, vol. 19, pp. 119–133, Jan. 2011.
- [4] C. C. Counselman, III, "Multipath-rejecting GPS antennas," *Proc. IEEE*, vol. 87, no. 1, pp. 86–91, Jan. 1999.
- [5] T. Q. Wu *et al.*, "A compact and broadband microstrip stacked patch antenna with circular polarization for 2.45 GHz mobile RFID reader," *IEEE Antennas Wireless Propag. Lett.*, vol. 12, pp. 623–626, 2013.
- [6] Y. Li and K.-M. Luk, "A multi-beam end-fire magneto-electric dipole antenna array for millimeter-wave applications," *IEEE Trans. Antennas Propag.*, vol. 64, no. 7, pp. 2894–2904, Jul. 2016.
- [7] Y. Li and K.-M. Luk, "60 GHz dual-polarized two-dimensional switch-beam wideband antenna array of aperture-coupled magneto-electric dipole," *IEEE Trans. Antennas Propag.*, vol. 64, no. 2, pp. 554–563, Feb. 2016.
- [8] Y. Li and K.-M. Luk, "A 60 GHz wideband circularly polarized aperture-coupled magneto-electric dipole antenna array," *IEEE Trans. Antennas Propag.*, vol. 64, no. 4, pp. 1325–1333, Apr. 2016.
- [9] Y. Lang, S.-W. Qu, and J.-X. Chen, "Wideband circularly polarized substrate integrated cavity-backed antenna array," *IEEE Antennas Wireless Propag. Lett.*, vol. 13, pp. 1513–1516, 2014.
- [10] H. Sun, Y.-X. Guo, and Z. Wang, "60 GHz circularly polarized U-slot patch antenna array on LTCC," *IEEE Trans. Antennas Propag.*, vol. 61, no. 1, pp. 430–435, Jan. 2013.
- [11] C. Liu, Y.-X. Guo, X. Bao, and S.-Q. Xiao, "60 GHz LTCC integrated circularly polarized helical antenna array," *IEEE Trans. Antennas Propag.*, vol. 60, no. 3, pp. 1329–1335, Mar. 2012.
- [12] B. Zhang, Y. P. Zhang, D. Titz, F. Ferrero, and C. Luxey, "A circularly-polarized array antenna using linearly-polarized sub grid arrays for highly-integrated 60 GHz radio," *IEEE Trans. Antennas Propag.*, vol. 61, no. 1, pp. 436–439, Jan. 2013.
- [13] A. B. Smolders and U. Johannsen, "The effect of phase and amplitude quantization on the axial ratio quality of mm-wave phased-arrays with sequential rotation," presented at the IEEE Int. Symp. Antennas Propag., Spokane, WA, USA, Jul. 2011.
- [14] M. F. Ismail *et al.*, "Dual-feed circular polarization compact array antenna," in *Proc. IEEE Asia-Pac. Conf. Appl. Electromagn.*, Dec. 2012, pp. 116–119.
- [15] J. Volakis, *Antenna Engineering Handbook*. New York, NY, USA: McGraw-Hill, 2009.
- [16] D. Sanchez-Escuderos, M. Ferrando-Bataller, J. Herranz, and V. M. Rodrigo-Peñarocha, "Low-loss circularly polarized periodic leaky-wave antenna," *IEEE Antennas Wireless Propag. Lett.*, vol. 15, pp. 614–617, 2016.
- [17] Q. Zhang, Q. Zhang, and Y. Chen, "Spoof surface plasmon polariton leaky-wave antennas using periodically loaded patches above PEC and AMC ground planes," *IEEE Antennas Wireless Propag. Lett.*, vol. 16, pp. 3014–3017, 2017.
- [18] F. L. Whetten and C. A. Balanis, "Meandering long slot leaky-wave waveguide-antennas," *IEEE Trans. Antennas Propag.*, vol. 39, no. 11, pp. 1553–1560, Nov. 1991.
- [19] J. Guo, Z. Li, J. Wang, M. Chen, and Z. Zhang, "Analysis and design of leaky-wave antenna with low SLL based on half-mode SIW structure," *Int. J. Antennas Propag.*, vol. 2015, 2015, Art. no. 570693.
- [20] A. A. Oliner and D. R. Jackson, "Leaky-wave antennas," in *Antenna Engineering Handbook*, J. L. Volakis, Ed., 4th ed. New York, NY, USA: McGraw-Hill, 2007, ch. 11.